

Somatomotor-Visual Resting State Functional Connectivity Increases After Two Years in the UK Biobank Longitudinal Cohort

Anton Orlichenko^a, Kuan-Jui Su^b, Qing Tian^b, Hui Shen^b, Hong-Wen Deng^b, and Yu-Ping Wang^a

^aDepartment of Biomedical Engineering, Tulane University, New Orleans, LA 70118

^bCenter for Biomedical Informatics and Genomics, School of Medicine, Tulane University, New Orleans, LA 70118

ABSTRACT

Purpose: Functional magnetic resonance imaging (fMRI) and functional connectivity (FC) have been used to follow aging in both children and older adults. Robust changes have been observed in children, where high connectivity among all brain regions changes to a more modular structure with maturation. In this work, we examine changes in FC in older adults after two years of aging in the UK Biobank longitudinal cohort.

Approach: We process data using the Power264 atlas, then test whether FC changes in the 2,722-subject longitudinal cohort are statistically significant using a Bonferroni-corrected t-test. We also compare the ability of Power264 and UKB-provided, ICA-based FC to determine which of a longitudinal scan pair is older. **Results:** We find a 6.8% average increase in SMT-VIS connectivity from younger to older scan (from $\rho = 0.39$ to $\rho = 0.42$) that occurs in male, female, older subject (> 65 years old), and younger subject (< 55 years old) groups. Among all inter-network connections, this average SMT-VIS connectivity is the best predictor of relative scan age, accurately predicting which scan is older 57% of the time. Using the full FC and a training set of 2,000 subjects, one is able to predict which scan is older 82.5% of the time using either the full Power264 FC or the UKB-provided ICA-based FC. **Conclusions:** We conclude that SMT-VIS connectivity increases in the longitudinal cohort, while resting state FC increases generally with age in the cross-sectional cohort. However, we consider the possibility of a change in resting state scanner task between UKB longitudinal data acquisitions.

Keywords: fMRI, functional connectivity, UK Biobank, longitudinal, cross-sectional, aging

1. INTRODUCTION

Functional magnetic resonance imaging (fMRI) is a non-invasive technique that has proven indispensable for investigating human neural processes in vivo.¹ For example, it has been used to localize the areas associated with vision,² attention,³⁴ emotion,⁵⁶⁷ and language⁸ to specific regions in the cortex, or at least find the regions that are most significantly involved in a specific task. Functional connectivity (FC) is a quantity derived from fMRI that measures the time correlation of blood oxygen level-dependent (BOLD) signal between different regions in the brain.⁹ FC has recently been used to predict age,¹⁰¹¹ sex,¹²¹³ race,¹⁴ psychiatric disease status,¹⁵¹⁶ and pre-clinical Alzheimer's disease.¹⁷ Efforts to predict general fluid intelligence, although common,¹⁸¹³ are thought by some to be confounded by differential achievement score distribution among ethnicities and the strong presence of race signal in FC.¹⁴ FC has proven effective in predictive studies because of its simplicity and its robust representation of complex BOLD signal activity, as evidenced by high subject identifiability across different scanner tasks and across time.¹⁹²⁰²¹

Besides being used as a predictive tool, FC has been observed to undergo changes throughout the lifespan. For example, connectivity in young children is generally very high between all brain regions and decreases while also becoming more modularized during and after puberty.²² The FC of males and females is also quantitatively

Further author information: (Send correspondence to Anton Orlichenko)
Anton Orlichenko: E-mail: aorlichenko@tulane.edu

41 different, with females having higher intra-DMN connectivity and males having relatively greater connectivity
42 between the DMN and other networks, although there is a wide degree of individual variation.^{23,24} Meanwhile,
43 studies have shown that changes occur in the DMN during late middle and old age,²⁵ although the exact
44 direction of change in FC does not always appear constant.²⁶ In addition, various studies have examined age-
45 related changes in the cingulum²⁷ and medial temporal lobe.²⁸ Given the recent interest in using fMRI to predict
46 pre-clinical Alzheimer’s disease,^{26,17} we believe a knowledge of ordinary changes in FC during old age is essential.
47 This is especially true because it has been shown that a confounder can easily be mistaken for a true signal
48 indicative of, e.g., general fluid intelligence or achievement score.¹⁴

49 This study uses the longitudinal cohort of the UKB²⁹ to examine changes in the FC of individuals after an
50 average of two years, the time between longitudinal scans. The UKB population of subjects with fMRI scans is
51 predominantly (98%) Caucasian, ruling out race as a possible confounding effect. Additionally, we investigate
52 changes in FC in longitudinal sub-populations based on subject age and sex. We find that average FC between
53 SMT-VIS networks increases on average from the first scan to the second, and that SMT and VIS-related
54 connectivities are more predictive of scan age than those of other networks. The complete FC, or a large subset,
55 is still required to attain the best accuracy.

56 2. METHODS

57 We first describe the UKB dataset and the longitudinal subset used for our analysis. We then describe pre-
58 processing of the fMRI data and conversion into FC. Finally, we discuss prediction of older vs younger scan in
59 the longitudinal cohort and detail our methods for analysis of FC changes.

60 2.1 UK Biobank Longitudinal Cohort

61 The UKB contains various data of more than 500,000 subjects in the UK, of who more than 40,000 have fMRI
62 scans.²⁹ We processed two longitudinal resting state scans for 2,722 subjects, taken approximately two years
63 apart. These subjects are approximately equally split between male and female, and have significant numbers of
64 younger and older adults. The longitudinal cohort is composed of 1,289 genetic males and 1,369 genetic females,
65 with the rest not having genetic sex information. The ethnicity of the subset of the UKB with fMRI scans is 98%
66 Caucasian. Besides the 2,722 subjects we processed, an additional 154 subjects have the second longitudinal scan
67 but not the first, resulting either from missing original source data or a failure in our SPM12-based preprocessing
68 pipeline.

69 2.2 fMRI Preprocessing

70 The original scan acquisition parameters are described elsewhere,^{30,31} but consist of both resting state and task
71 fMRI scans with a repetition time of $TR = 0.735$ sec. For this study, we examined the resting state scans
72 only. All resting state 4D fMRI volumes were processed with SPM12, including co-registration and warping to
73 MNI space (<http://www.fil.ion.ucl.ac.uk/spm/software/spm12/>). BOLD signal was extracted using the
74 Power264 atlas,³² which consists of 264 ROIs grouped into 14 functional networks and represented by 5mm
75 radius spheres. The resulting timeseries were bandpass filtered between 0.01 and 0.15 Hz to remove scanner
76 drift, noise, heartbeat, and some breathing signal. Pearson correlation of the filtered timeseries was used to
77 create subject-specific FC matrices, which were reduced to the unique entries in the upper right triangle and
78 vectorized. The entire procedure is summarized in Figure 1.

79 In contrast to the Power264 atlas-derived FC constructed by us, the original UKB data provided the unique
80 part of 21-region and 55-region FC and partial correlation-based connectivity (PC) matrices based on ICA in
81 vectorized format.³⁰ These matrices were calculated through the use of PCA on whole cohort fMRI data followed
82 by ICA,³⁰ meaning that regions overlap in an unpredictable way and are not associated with specific functional
83 networks. Although prediction using 55-component ICA-based FC and PC is often as good as and sometimes
84 better than prediction using Power264 atlas-derived FC, the resulting connectivities are uninterpretable with
85 regards to BOLD signal within specific regions. Additionally, in predicting which scan is older, Power264
86 asymptotes to a higher predictive accuracy than either of the ICA-derived measures (see Figure 4).

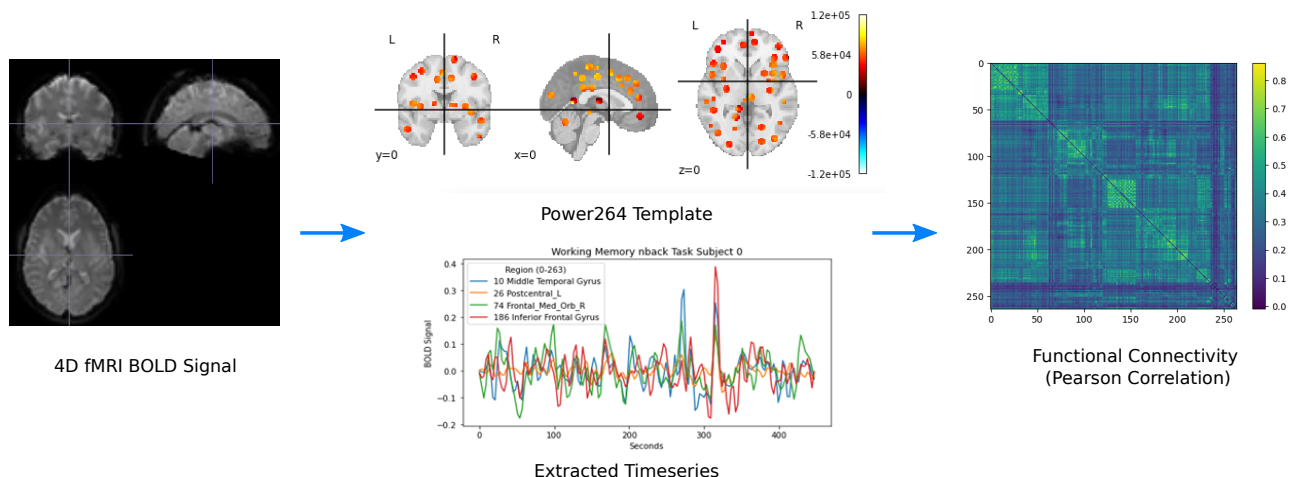


Figure 1. Preprocessing pipeline for converting 4D fMRI volumes into FC using the Power264 atlas.³² Reproduced with permission from Orlichenko et al. (2023).³³

2.3 Prediction of Scan Order and Analysis of FC

Prediction of scan age in the UKB longitudinal cohort was carried out by logistic regression (<https://scikit-learn.org/stable/>) models with 20 bootstrapping repetitions, using the scikit-learn implementation.³⁴ The regularization parameter was fixed to $C = 1$, which was found to be near the optimal value for all training set sizes using grid search. It was found that a simple difference of scan FCs gave the best prediction results compared to concatenation or difference and concatenation, using either logistic regression or MLP. The training set was created with randomization of whether older scan was subtracted from younger scan or younger scan was subtracted from older scan. Our code for computing prediction accuracy can be found online (<https://github.com/aorliche/ukb-longitudinal-smt-vis>). However, UKB data sharing policy precludes us from posting the longitudinal data itself; interested researchers may contact us with any questions.

Analysis of FC was performed by finding the mean (Figure 2) and standard deviation (Figure 9) of older scan FC minus younger scan FC for the longitudinal cohort. Additionally, prediction of scan order was carried out using the average connectivity between each of the Power264 networks, each network consisting of many individual ROIs. As before, logistic regression with 20 bootstrap repetitions and $C = 1$ was used for this purpose. A Bonferroni-corrected two-sided t-test was applied to the 105 average inter-network connectivity differences (from the complete graph of 14 functional networks) of the 2,722 longitudinal subjects to determine if they were significantly different from zero (Figure 5 Bottom).

3. RESULTS

We first describe trends in FC changes during the average of 2 years between longitudinal scans, summarize the ability of simple machine learning models to identify older vs younger scan, and investigate the ability of specific inter-network connectivities to predict scan order. We then summarize the statistical significance of inter-network FC changes with aging, in both the longitudinal and cross-sectional cohorts of the UKB. Finally, we consider the possibility that the observed longitudinal changes are due to a change in scanner task by presenting inter-task FC differences in the Philadelphia Neurodevelopmental Cohort (PNC) dataset.³⁵

3.1 Inter-Network FC Changes

In Figure 2, we show that, on average, SMT-VIS connectivity increases from younger scan to older scan. The right hand side of Figure 2 displays divisions of the 14 functional networks included in the Power264 atlas. Network labels and abbreviations are listed in Table 1. The increase in connectivity is large and distinct over the majority of SMT-VIS FCs compared to other non-SMT and non-VIS FCs. Many FCs involving the VIS network appear to increase in connectivity from the first scan to the second. The average change in FC in the

Older Scan FC Minus Younger Scan FC (Mean of All Subjects)

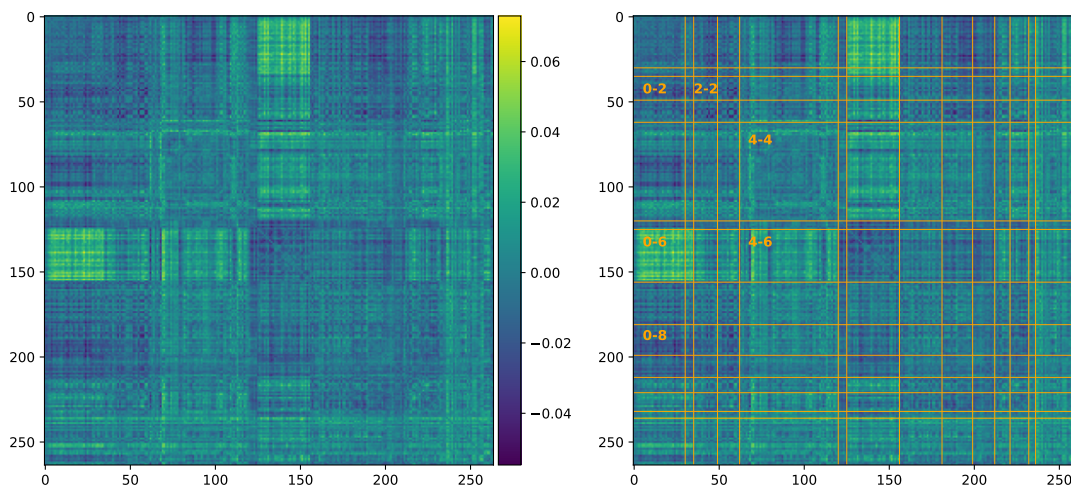


Figure 2. Difference in FC calculated by older scan minus younger scan, averaged over all 2,722 longitudinal cohort subjects. There are significant average differences in SMT-VIS connectivity (labeled 0-6). The same plot is displayed on the left and right, with Power264 network divisions on the right hand side. Network labels can be found in Table 1.

Table 1. Regions, abbreviations, and labels in the Power264 atlas.

Functional Networks

| Label | ROIs | | Label | ROIs | |
|-------|---------|-------------------------|-------|---------|--------------------------|
| 0 | 0-29 | Somatomotor Hand (SMT) | 7 | 156-180 | Frontoparietal (FRNT) |
| 1 | 30-34 | Somatomotor Mouth (SMT) | 8 | 181-198 | Saliency (SAL) |
| 2 | 35-48 | Cinguloopercular (CNG) | 9 | 199-211 | Subcortical (SUB) |
| 3 | 49-61 | Auditory (AUD) | 10 | 212-220 | Ventral Attention (VTRL) |
| 4 | 62-119 | Default Mode (DMN) | 11 | 221-231 | Dorsal Attention (DRSL) |
| 5 | 120-124 | Memory (MEM) | 12 | 232-235 | Cerebellar (CB) |
| 6 | 125-155 | Visual (VIS) | 13 | 236-263 | Uncertain (UNK) |

117 SMT-VIS connection is 6.8%, corresponding to a mean change $\mu_{\Delta\rho} = +0.03$, compared to a standard deviation
 118 of $\sigma_{\Delta\rho} = 0.26$. Figure 5 shows that, although small compared to the standard deviation, this difference is very
 119 significant.

120 Figure 3 displays the same analysis, i.e., the average change from first scan to second, for four subsets of the
 121 cohort. These subsets are male subjects, female subjects, young (< 55 years old) subjects, and old (> 65 years
 122 old) subjects. All four subsets observed the same effect as the whole cohort, thus we rule out very old age or
 123 gender as confounding factors.

124 3.2 Predicting Older Scan of Pair

125 In Figure 4, one can see that is possible to predict which scan of a longitudinal pair is older with the Power264
 126 atlas at an accuracy of 82.5%, having 2,000 subjects in the training set and the rest in the test set. This
 127 measurement was repeated with 20 bootstrap iterations and averaged. The entire 34,716-feature upper right
 128 triangle of the FC matrix was used to make the prediction. One can also see that the ICA FC/PC matrices
 129 provided pre-processed along with the UKB data are also able to predict scan order, although at a slightly
 130 reduced accuracy. Prediction is possible at an accuracy of 60-70% using only 100-200 training set subjects.

Older Scan FC Minus Younger Scan FC (By Group)

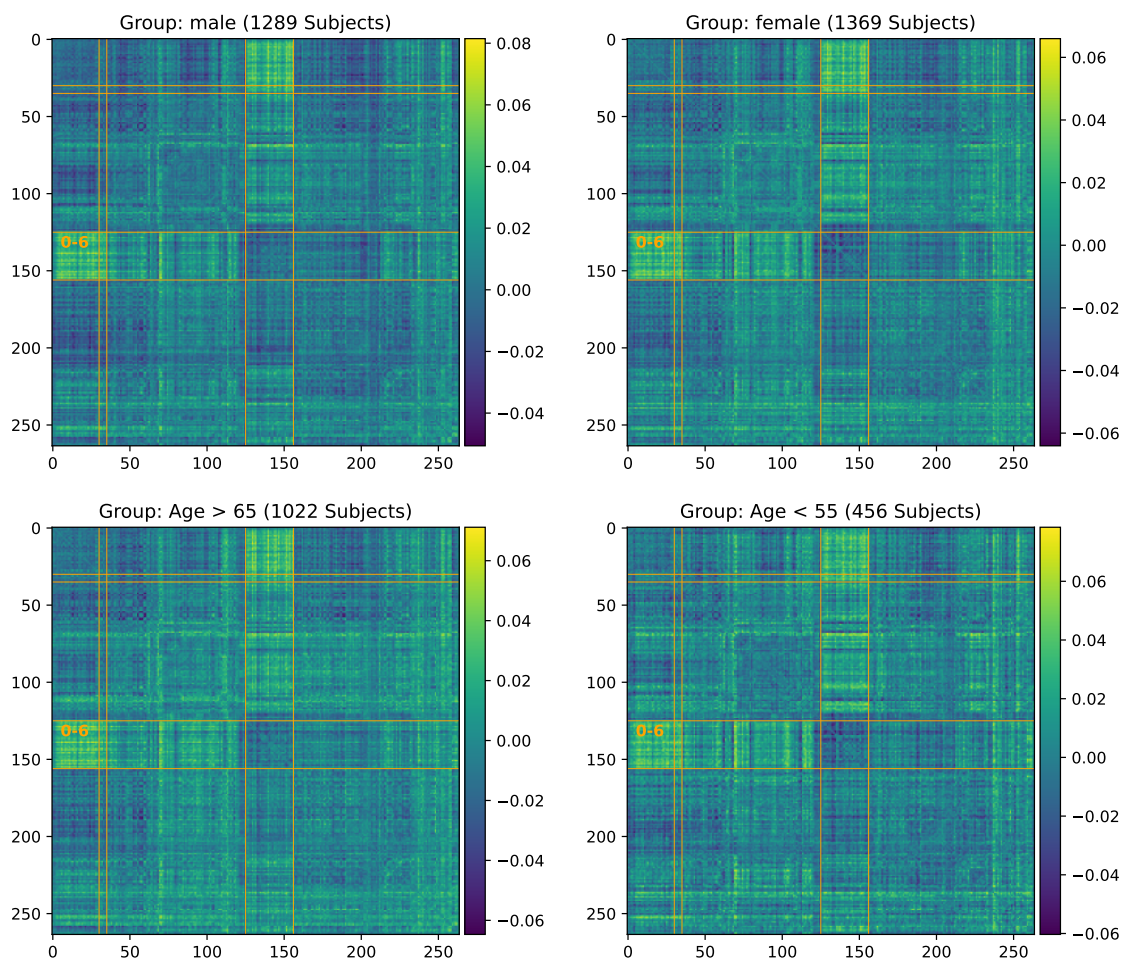


Figure 3. Significant increase in SMT-VIS connectivity after an average of 2 years in the UKB longitudinal cohort appears in male, female, younger, and older groups, and seems to be an invariant feature of FC change in the longitudinal UKB cohort.

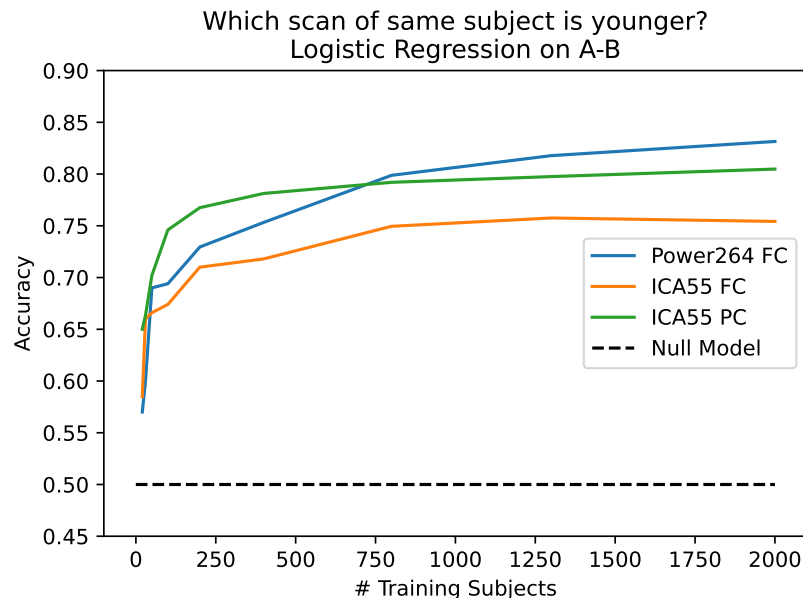


Figure 4. Capability of predicting older scan of a pair based on the difference of FC between the two scans, as a function of the number of training subjects. Three inputs are used: 55 component ICA FC, 55 component ICA PC, and the Power264 atlas FC. Prediction accuracy asymptotes at 82.5%.

Table 2. Number of subjects in the longitudinal cohort increasing and decreasing in average FC within the SMT-VIS connection and within the whole brain.

| Group | +SMT-VIS FC | -SMT-VIS FC | +Total FC | -Total FC | Total Subjects |
|----------------|-------------|-------------|-------------|-----------|----------------|
| Male | 778 (60.4%) | 511 | 690 (53.5%) | 599 | 1289 |
| Female | 741 (54.1%) | 628 | 671 (49.0%) | 698 | 1369 |
| < 55 years old | 269 (59.0%) | 187 | 249 (54.6%) | 207 | 456 |
| > 65 years old | 577 (56.5%) | 445 | 520 (50.1%) | 502 | 1022 |

131 3.3 Prediction of Older Scan Using Specific Inter-Network Connections

132 In Figure 5, we rank average inter-network FCs in their ability to predict scan order. As expected from the mean
 133 change in FC (Figure 2), the SMT-VIS connection is the most predictive of longitudinal scan age. Furthermore,
 134 SMT and VIS networks are included among the next several most predictive inter-network connections. In
 135 Figure 5 bottom, we plot the predictive ability of all 105 inter-network connections, along with a p-value for the
 136 inter-network FC change being significantly different from zero. The raw p-value has been multiplied by 105
 137 to account for multiple comparisons. It is highly significant for the first 10 or so most predictive inter-network
 138 connections.

139 Table 3.3 lists the number of subjects whose FC increased or decreased for the SMT-VIS connection and over
 140 the entire brain. The table is divided among the four subsets of the longitudinal cohort mentioned previously.
 141 Additionally, we correlated several dozen subject phenotypes and longitudinally-tracked variables with changes
 142 in FC and report the most significant in Appendix B. In that section, we find an interesting but small correlation
 143 with hand grip strength, body mass index (BMI), and basal metabolic rate. In Section 3.4, we find that average
 144 resting state FC increases with age across most inter-network connections in the much larger UKB cross-sectional
 145 cohort.

146 3.4 FC Changes with Age in the UKB Cross-Sectional Cohort

147 We find that average resting state FC has a significant increase in almost all inter-network connections in the
 148 UKB cross-sectional cohort. Average maps of FC change are shown in Figure 7. We fail to find a higher SMT-VIS

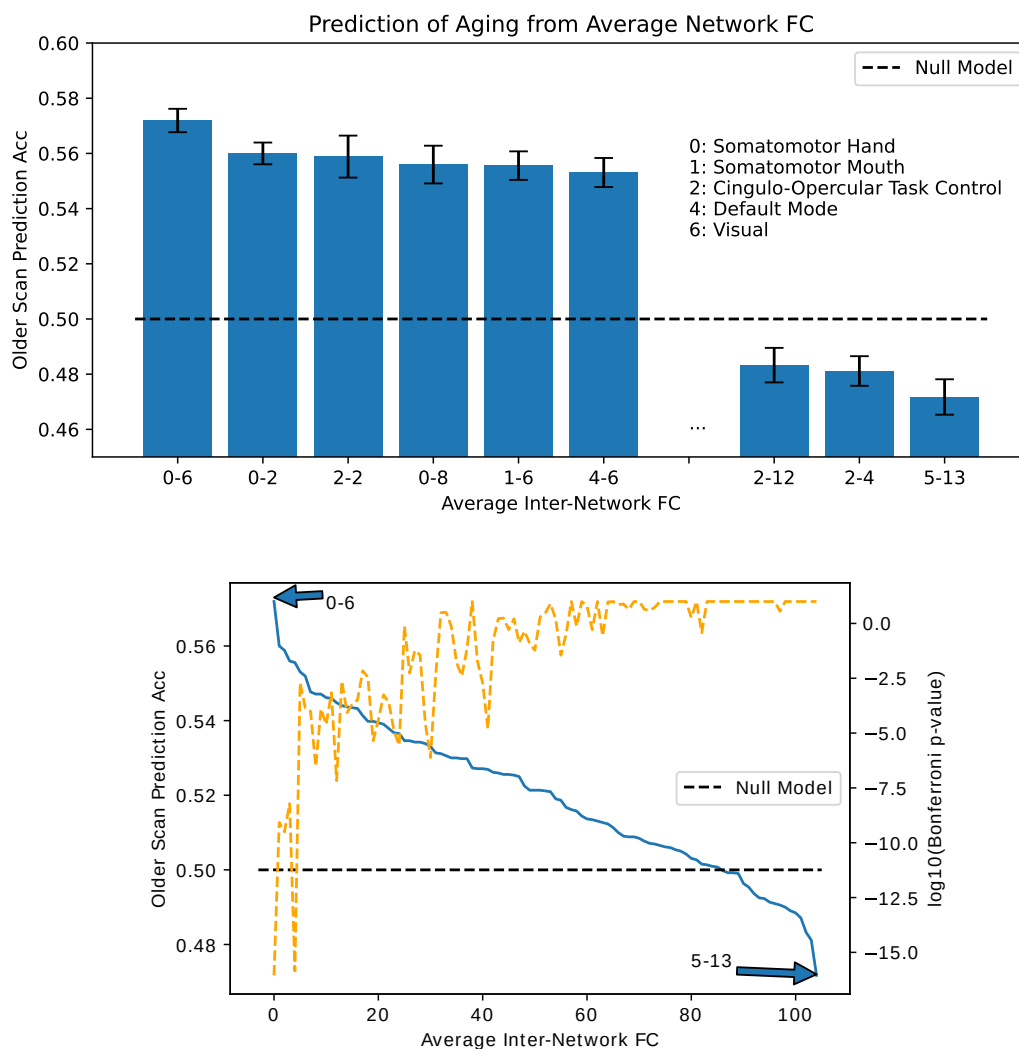


Figure 5. Ability to predict which scan of a subject is older based on average connectivity between regions. Top: best and worst inter-network connectivities for prediction. Bottom: Prediction accuracy for all 105 inter-network connectivities. We find that SMT-VIS connectivity has the maximum predictive ability of all regions at 57%. In general, network-level connectivities involving SMT and VIS networks have higher predictive ability compared to other regions. The dashed orange line displays negative log base 10 of the Bonferroni-corrected p-value for significance of FC change between scans.

Power264 Atlas Visual and Somatomotor Regions

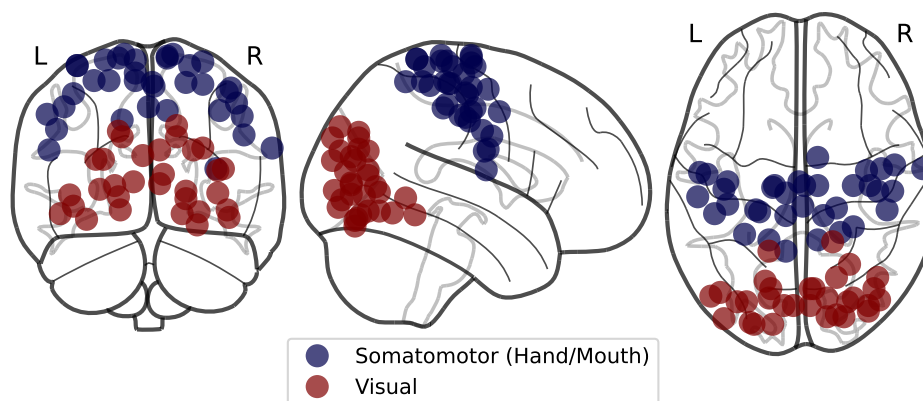


Figure 6. SMT and VIS regions in the Power264 atlas.

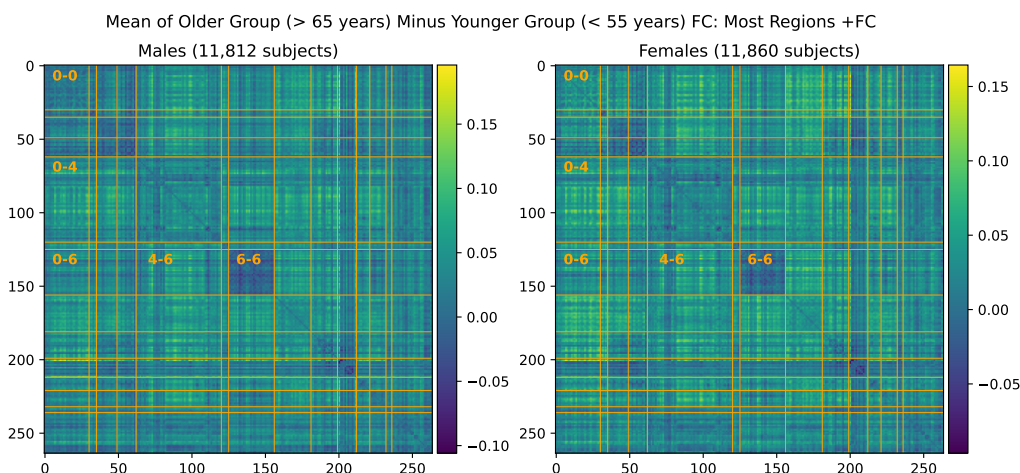


Figure 7. Mean FC change from younger group to older group in the large UKB cross-sectional cohort.

149 change compared to other connections; however, almost all inter-network regions have a large positive increase
 150 in FC with aging. We give precise numbers for four inter-network connections as well as total FC in Table 3.

151 In total, there are 9,387 older males (> 65 years old), 2,425 younger males (< 55 years old), 8,728 older
 152 females (> 65 years old), and 3,132 younger females (< 55 years old) in the UKB cross-sectional cohort.

153 3.5 Comparison with FC Differences Between Scanner Tasks in the PNC Dataset

154 We consider the possibility that the difference in SMT-VIS connectivity between the two scans of the longitudinal
 155 cohort is due to a change in scanner task. In Figure 8, we show the average FC differences between 3 different
 156 scanner tasks in the PNC dataset.³⁵ This dataset contains 1,345 children and young adults having all of three different
 157 scanner tasks: resting state, working memory, and emotion identification. The preprocessing and FC creation
 158 steps for this dataset have been described elsewhere.¹⁰ We note that the VIS-VIS is most different for change
 159 in task, but that the SMT-VIS is not qualitatively more different than the rest of FC. Also, the magnitude of
 160 change in FC in the PNC dataset between tasks is much larger than in the UKB longitudinal cohort.

Table 3. Average FC changes with aging in the UKB cross-sectional cohort from young subjects (< 55 years old) to old subjects (> 65 years old).

| Regions | Male (Young to Old) | | | Female (Young to Old) | | |
|---------------|---------------------|-------------------|--------------|-----------------------|-------------------|--------------|
| | FC Increase | Std Dev of Avg FC | p-value | FC Increase | Std Dev of Avg FC | p-value |
| SMT-VIS (0-6) | 0.031 | 0.13 | $< 10^{-23}$ | 0.029 | 0.13 | $< 10^{-25}$ |
| SMT-DMN (0-4) | 0.045 | 0.11 | $< 10^{-78}$ | 0.043 | 0.11 | $< 10^{-82}$ |
| DMN-VIS (4-6) | 0.042 | 0.11 | $< 10^{-60}$ | 0.035 | 0.11 | $< 10^{-52}$ |
| VIS-VIS (6-6) | -0.014 | 0.10 | $< 10^{-7}$ | -0.009 | 0.11 | < 0.002 |
| Total FC | 0.035 | 0.09 | $< 10^{-64}$ | 0.031 | 0.087 | $< 10^{-62}$ |

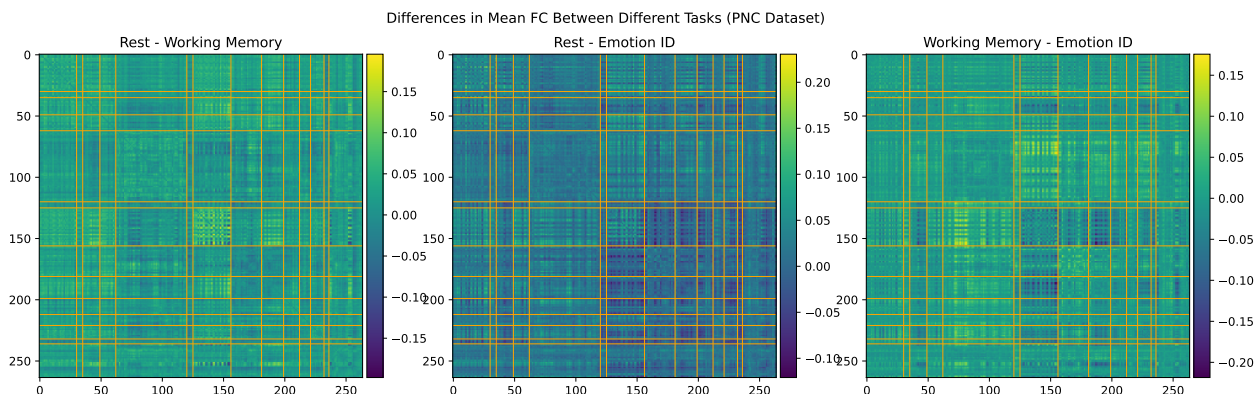


Figure 8. Average differences in FC between three scanner tasks of 1,345 subjects in the PNC dataset. This is a cross-sectional, not longitudinal, dataset.

4. DISCUSSION

161
 162 Farràs-Permanyer et al. (2019)³⁶ find that mean resting state FC may increase throughout the entire brain for
 163 the oldest subject (> 80 years old) group. As shown in Appendix A, we confirm a small, statistically insignificant
 164 increase in total longitudinal FC in the healthy controls of the ADNI dataset,³⁷ another elderly population with
 165 multiple longitudinal fMRI scans. In Section 3.4, we show that there is a large, statistically significant increase
 166 in average resting state FC across almost all inter-network connections in the UKB cross-sectional cohort with
 167 increased age. This cross-sectional cohort is much larger than the longitudinal cohort we describe in the main part
 168 of this paper. The fact that SMT-VIS FC also increases in the cross-sectional cohort, but not disproportionately
 169 compared to the rest of FC, raises the possibility of a change in resting state scanner task during the second
 170 longitudinal scan. We believe this longitudinal change is not an artifact of our pre-processing methods. Credence
 171 should increase in our pre-processing methods since the UKB-provided ICA-based FC and PC is also able to
 172 predict longitudinal scan ordering at almost the same level as our Power264-based approach, although the ICA
 173 FC and PC matrices are not interpretable.

174 Many studies have focused on examining connectivity in the DMN associated with aging.^{38,39} These studies
 175 find areas of increased connectivity as well as areas of decreased connectivity. There are two problems with such
 176 studies. First, they are for the most part cross-sectional and do not follow a single subject across a multi-year
 177 period. Second, they mostly use small numbers of subjects, the majority of studies enrolling fewer than 50,
 178 making it impossible to identify small effects. On the other hand, one study performed on a cohort of more than
 179 2,000 older subjects in Rotterdam found age-related changes in connectivity to be complicated, drawing no firm
 180 conclusions.⁴⁰ We note that the Rotterdam study was not longitudinal but cross-sectional.

181 We conjecture the fact that most studies only focus on DMN and report decreased connectivity³⁸ in aging
 182 populations may be related to the large number of ROIs in the DMN and an implicit bias inherent in the word
 183 “connectivity.” Naturally, as we reach very old age we expect physical connections to degenerate, not become

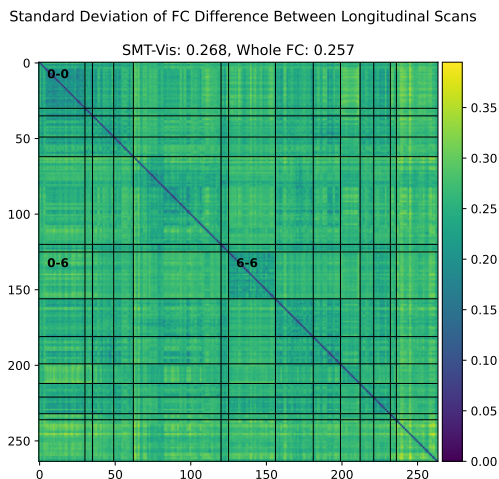


Figure 9. Standard deviation of difference between older scan FC and younger scan FC in the UKB longitudinal cohort. Note that the magnitude of average standard deviation (0.26) of SMT-VIS connectivity change is large compared to mean SMT-VIS connectivity change (0.03). However, we show in Figure 5 that this connectivity change is highly statistically significant. The smallest average standard deviations are found in SMT-SMT (0.2) and VIS-VIS (0.22) connectivities.

184 stronger. In fact, FC is really the synchronization of BOLD signal between regions, and does not imply a direct
185 physical link between regions. Young children are known to have higher average FC than young adults;²²⁴¹ thus
186 older subjects may be reverting to a less optimal state as they age.

187 On the other hand, as we describe in Appendix B, physical observables such as hand grip strength in the
188 UKB longitudinal cohort are weakly correlated with an increase in FC in SMT-CB and VIS-CB connectivity.
189 Additionally, we find BMI and basal metabolic rate are weakly correlated with the longitudinal increase in SMT-
190 VIS connectivity (see Appendix B). This may suggest a small health related effect that is found throughout the
191 study cohort and includes male, female, younger, and older subjects. Finally, as discussed in Section 3.5, we
192 cannot rule out the possibility that changes in longitudinal FC are caused by a change in scanner task between
193 acquisition of the two longitudinal timepoints.

194 We show in this work that the average connectivity increase in the SMT-VIS connection is small but highly
195 statistically significant. The average change in FC in this connection is only 6.8%, corresponding to a mean
196 change $\mu_{\Delta\rho} = +0.03$, compared to a standard deviation of change from subject to subject of $\sigma_{\Delta\rho} = 0.26$ (see
197 Figure 9). However, using our longitudinal sample of 2,722 subjects, we find the average SMT-VIS connectivity
198 change from younger scan to older scan is significant as level of $p < 10^{-15}$ after Bonferroni correction for
199 multiple comparisons (Figure 5). Finding such small effects is helped by the use of large number of subjects and
200 longitudinal data.

201 5. CONCLUSION

202 In this work, we pre-process a 2,722 subject longitudinal subset of the UK Biobank dataset and examine FC
203 using the Power264 atlas. We find that in scans taken an average of two years apart, the average functional
204 connectivity between SMT and VIS network regions tends to increase. This occurs in male, female, younger
205 (< 55 years old), and older (> 65 years old) subjects. We verify the ability of this average FC increase to
206 predict scan ordering using simple machine learning models. The identification of an increase in connectivity
207 with non-pathological aging, in longitudinal as well as cross-sectional cohorts, and specifically in the SMT-VIS
208 synchronization of BOLD signal, may lead to novel insights about brain function in old age. Additionally,
209 we identify an effect that could possibly show up as a confounder in studies of dementia or neurodegenerative
210 diseases. Nonetheless, we remain open to the idea of a change in resting state scanner task during acquisition of
211 the longitudinal data in the UKB being partly responsible for this effect.

DISCLOSURES

212

213 The authors have no conflicts of interest to report.

CODE AND DATA AVAILABILITY

214

215 fMRI and phenotype data came from the UK Biobank (application ID 61915), available via application to
216 qualified researchers. Additional data used in Appendix A came from the Alzheimer’s Disease Network Initiative
217 (ADNI), available via application from <https://adni.loni.usc.edu/>. Additional neuroimaging data came from
218 the Neurodevelopmental Genomics: Trajectories of Complex Phenotypes database of genotypes and phenotypes
219 repository, dbGaP Study Accession ID phs000607.v3.p2.

220 All code used in this study is available from GitHub at [https://github.com/aorliche/ukb-longitudinal-](https://github.com/aorliche/ukb-longitudinal-smt-vis)
221 [smt-vis](https://github.com/aorliche/ukb-longitudinal-smt-vis). We do not have permission to post original subject data; however, it may be obtained via application
222 from the sources listed above.

ACKNOWLEDGMENTS

223

224 The authors would like acknowledge the NIH (grants R01 GM109068, R01 MH104680, R01 MH107354, P20
225 GM103472, R01 EB020407, R01 EB006841, R56 MH124925) and NSF (#1539067) for partial funding support.

226 This research was supported in part using high performance computing (HPC) resources and services provided
227 by Information Technology at Tulane University, New Orleans, LA.

Biography

228

229 **Anton Orlichenko** received his B.S. in Electrical and Computer Engineering in 2010 from the Illinois Institute
230 of Technology. He is currently a Ph.D. candidate at Tulane University, working on mathematical models of brain
231 function and genetics.

232 **Kuan-Jui Su** received his Ph.D. from Tulane University School of Medicine in 2023. He currently works at
233 the Center for Biomedical Informatics and Genomics at Tulane University.

234 **Qing Tian** holds an M.S. degree and works with Dr. Deng and Dr. Shen as the database administrator for
235 the Center for Biomedical Informatics and Genomics at Tulane University.

236 **Hui Shen** received his B.S. from the University of Science and Technology in China and his Ph.D. from
237 Creighton University. He is currently a geneticist at the Center for Biomedical Informatics and Genomics at
238 Tulane University.

239 **Hong-Wen Deng** received his B.S. and M.S. from Peking University. He received a further M.S. and Ph.D.
240 degrees from the University of Oregon. He currently runs the Center for Biomedical Informatics and Genomics
241 at the Tulane University School of Medicine.

242 **Yu-Ping Wang** received his B.S. from Tianjin University in 1990, and his M.S. and PhD degrees from
243 Xian Jiaotong University in 1993 and 1996, respectively. He currently runs the Multiscale Bioimaging and
244 Bioinformatics Lab at Tulane University.

REFERENCES

245

- 246 [1] Belliveau, J. W., Kennedy, D. N., McKinstry, R. C., Buchbinder, B. R., Weisskoff, R. M., Cohen, M. S.,
247 Vevea, J. M., Brady, T. J., and Rosen, B. R., “Functional mapping of the human visual cortex by magnetic
248 resonance imaging,” *Science* **254** **5032**, 716–9 (1991).
- 249 [2] Cox, D. D. and Savoy, R. L., “Functional magnetic resonance imaging (fMRI) “brain reading”: detecting
250 and classifying distributed patterns of fMRI activity in human visual cortex,” *Neuroimage* **19**, 261–270
251 (June 2003).
- 252 [3] Coull, J. T. and Nobre, A. C., “Where and when to pay attention: the neural systems for directing attention
253 to spatial locations and to time intervals as revealed by both PET and fMRI,” *J. Neurosci.* **18**, 7426–7435
254 (Sept. 1998).

- 255 [4] Pugh, K. R., Shaywitz, B. A., Shaywitz, S. E., Fulbright, R. K., Byrd, D., Skudlarski, P., Shankweiler,
256 D. P., Katz, L., Constable, R. T., Fletcher, J., Lacadie, C., Marchione, K., and Gore, J. C., “Auditory
257 selective attention: An fMRI investigation,” *Neuroimage* **4**, 159–173 (Dec. 1996).
- 258 [5] Phan, K. L., Wager, T., Taylor, S. F., and Liberzon, I., “Functional neuroanatomy of emotion: a meta-
259 analysis of emotion activation studies in PET and fMRI,” *Neuroimage* **16**, 331–348 (June 2002).
- 260 [6] Ochsner, K. N., Bunge, S. A., Gross, J. J., and Gabrieli, J. D. E., “Rethinking feelings: An fmri study of
261 the cognitive regulation of emotion,” *Journal of Cognitive Neuroscience* **14**(8), 1215–1229 (2002).
- 262 [7] Koelsch, S., Fritz, T., Cramon, V. D. Y., Müller, K., and Friederici, A. D., “Investigating emotion with
263 music: an fMRI study,” *Hum. Brain Mapp.* **27**, 239–250 (Mar. 2006).
- 264 [8] Hernandez, A. E., Dapretto, M., Mazziotta, J., and Bookheimer, S., “Language switching and language
265 representation in Spanish-English bilinguals: an fMRI study,” *Neuroimage* **14**, 510–520 (Aug. 2001).
- 266 [9] van den Heuvel, M. P. and Hulshoff Pol, H. E., “Exploring the brain network: a review on resting-state
267 fMRI functional connectivity,” *Eur. Neuropsychopharmacol.* **20**, 519–534 (Aug. 2010).
- 268 [10] Orlichenko, A., Qu, G., Zhang, G., Patel, B., Wilson, T. W., Stephen, J. M., Calhoun, V. D., and Wang,
269 Y.-P., “Latent similarity identifies important functional connections for phenotype prediction,” *IEEE Trans-*
270 *actions on Biomedical Engineering* **70**(6), 1979–1989 (2023).
- 271 [11] Hu, W., Cai, B., Zhang, A., Calhoun, V. D., and Wang, Y.-P., “Deep collaborative learning with application
272 to the study of multimodal brain development,” *IEEE Transactions on Biomedical Engineering* **66**(12),
273 3346–3359 (2019).
- 274 [12] İçer, S., İrem Acer, and Baş, A., “Gender-based functional connectivity differences in brain networks in
275 childhood,” *Computer Methods and Programs in Biomedicine* **192**, 105444 (2020).
- 276 [13] Sen, B. and Parhi, K. K., “Predicting biological gender and intelligence from fmri via dynamic functional
277 connectivity,” *IEEE Transactions on Biomedical Engineering* **68**(3), 815–825 (2021).
- 278 [14] Orlichenko, A., Daly, G., Liu, A., Shen, H., Deng, H.-W., and Wang, Y.-P., “ImageNomer: developing an
279 fMRI and omics visualization tool to detect racial bias in functional connectivity,” (2023).
- 280 [15] Wang, S., Zhan, Y., Zhang, Y., Lyu, L., Lyu, H., Wang, G., Wu, R., Zhao, J., and Guo, W., “Abnormal
281 long- and short-range functional connectivity in adolescent-onset schizophrenia patients: A resting-state
282 fMRI study,” *Progress in Neuro-Psychopharmacology and Biological Psychiatry* **81**, 445–451 (Feb. 2018).
- 283 [16] Rashid, B., Arbabshirani, M. R., Damaraju, E., Cetin, M. S., Miller, R., Pearlson, G. D., and Calhoun,
284 V. D., “Classification of schizophrenia and bipolar patients using static and dynamic resting-state fMRI
285 brain connectivity,” *Neuroimage* **134**, 645–657 (July 2016).
- 286 [17] Millar, P. R., Luckett, P. H., Gordon, B. A., and Benzinger, T. L., “Predicting brain age from functional
287 connectivity in symptomatic and preclinical alzheimer disease,” *NeuroImage* **256**, 119228 (2022).
- 288 [18] Qu, G., Xiao, L., Hu, W., Wang, J., Zhang, K., Calhoun, V. D., and ping Wang, Y., “Ensemble manifold
289 regularized multi-modal graph convolutional network for cognitive ability prediction,” *IEEE Transactions*
290 *on Biomedical Engineering* **68**, 3564–3573 (2021).
- 291 [19] Finn, E. S., Shen, X., Scheinost, D., Rosenberg, M. D., Huang, J., Chun, M. M., Papademetris, X., and
292 Constable, R. T., “Functional connectome fingerprinting: identifying individuals using patterns of brain
293 connectivity,” *Nat. Neurosci.* **18**, 1664–1671 (Nov. 2015).
- 294 [20] Cai, B., Zhang, G., Hu, W., Zhang, A., Zille, P., Zhang, Y., Stephen, J. M., Wilson, T. W., Calhoun, V. D.,
295 and Wang, Y.-P., “Refined measure of functional connectomes for improved identifiability and prediction,”
296 *Hum. Brain Mapp.* **40**, 4843–4858 (Nov. 2019).
- 297 [21] Orlichenko, A., Qu, G., Zhou, Z., Ding, Z., and Wang, Y.-P., “Angle basis: A generative model and
298 decomposition for functional connectivity,” (2023).
- 299 [22] Dosenbach, N. U. F., Nardos, B., Cohen, A. L., Fair, D. A., Power, J. D., Church, J. A., Nelson, S. M., Wig,
300 G. S., Vogel, A. C., Lessov-Schlaggar, C. N., Barnes, K. A., Dubis, J. W., Feczko, E., Coalson, R. S., Pruett,
301 Jr, J. R., Barch, D. M., Petersen, S. E., and Schlaggar, B. L., “Prediction of individual brain maturity using
302 fMRI,” *Science* **329**, 1358–1361 (Sept. 2010).
- 303 [23] Mak, L. E., Minuzzi, L., MacQueen, G., Hall, G., Kennedy, S. H., and Milev, R., “The default mode network
304 in healthy individuals: A systematic review and meta-analysis,” *Brain Connect.* **7**, 25–33 (Feb. 2017).

- 305 [24] Ficek-Tani, B., Horien, C., Ju, S., Xu, W., Li, N., Lacadie, C., Shen, X., Scheinos, D., Constable, T.,
306 and Fredericks, C., “Sex differences in default mode network connectivity in healthy aging adults,” *Cereb.*
307 *Cortex* (Dec. 2022).
- 308 [25] Fjell, A. M., Sneve, M. H., Grydeland, H., Storsve, A. B., Amlien, I. K., Yendiki, A., and Walhovd,
309 K. B., “Relationship between structural and functional connectivity change across the adult lifespan: A
310 longitudinal investigation,” *Hum. Brain Mapp.* **38**, 561–573 (Jan. 2017).
- 311 [26] Staffaroni, A. M., Brown, J. A., Casaletto, K. B., Elahi, F. M., Deng, J., Neuhaus, J., Cobigo, Y., Mumford,
312 P. S., Walters, S., Saloner, R., Karydas, A., Coppola, G., Rosen, H. J., Miller, B. L., Seeley, W. W., and
313 Kramer, J. H., “The longitudinal trajectory of default mode network connectivity in healthy older adults
314 varies as a function of age and is associated with changes in episodic memory and processing speed,” *J.*
315 *Neurosci.* **38**, 2809–2817 (Mar. 2018).
- 316 [27] Hirsiger, S., Koppelmans, V., Méritat, S., Liem, F., Erdeniz, B., Seidler, R. D., and Jäncke, L., “Structural
317 and functional connectivity in healthy aging: Associations for cognition and motor behavior,” *Hum. Brain*
318 *Mapp.* **37**, 855–867 (Mar. 2016).
- 319 [28] Salami, A., Wählin, A., Kaboodvand, N., Lundquist, A., and Nyberg, L., “Longitudinal evidence for disso-
320 ciation of anterior and posterior MTL resting-state connectivity in aging: Links to perfusion and memory,”
321 *Cereb. Cortex* **26**, 3953–3963 (Oct. 2016).
- 322 [29] Sudlow, C., Gallacher, J., Allen, N., Beral, V., Burton, P., Danesh, J., Downey, P., Elliott, P., Green, J.,
323 Landray, M., Liu, B., Matthews, P., Ong, G., Pell, J., Silman, A., Young, A., Sprosen, T., Peakman, T.,
324 and Collins, R., “UK biobank: An open access resource for identifying the causes of a wide range of complex
325 diseases of middle and old age,” *PLoS Med.* **12**, e1001779 (Mar. 2015).
- 326 [30] Smith, S. M., Alfaro-Almagro, F., and Miller, K. L., “Uk biobank brain imaging documentation,” tech. rep.,
327 UK Biobank (September 2022).
- 328 [31] Alfaro-Almagro, F., Jenkinson, M., Bangerter, N. K., Andersson, J. L. R., Griffanti, L., Douaud, G.,
329 Sotiropoulos, S. N., Jbabdi, S., Hernandez-Fernandez, M., Vallee, E., Vidaurre, D., Webster, M., McCarthy,
330 P., Rorden, C., Daducci, A., Alexander, D. C., Zhang, H., Dragonu, I., Matthews, P. M., Miller, K. L., and
331 Smith, S. M., “Image processing and quality control for the first 10,000 brain imaging datasets from UK
332 biobank,” *Neuroimage* **166**, 400–424 (Feb. 2018).
- 333 [32] Power, J. D., Cohen, A. L., Nelson, S. M., Wig, G. S., Barnes, K. A., Church, J. A., Vogel, A. C., Laumann,
334 T. O., Miezin, F. M., Schlaggar, B. L., and Petersen, S. E., “Functional network organization of the human
335 brain,” *Neuron* **72**, 665–678 (Nov. 2011).
- 336 [33] Orlichenko, A., Qu, G., Su, K.-J., Liu, A., Shen, H., Deng, H.-W., and Wang, Y.-P., “Identifiability in
337 Functional Connectivity May Unintentionally Inflate Prediction Results,” (8 2023).
- 338 [34] Pedregosa, F., Varoquaux, G., Gramfort, A., Michel, V., Thirion, B., Grisel, O., Blondel, M., Prettenhofer,
339 P., Weiss, R., Dubourg, V., Vanderplas, J., Passos, A., Cournapeau, D., Brucher, M., Perrot, M., and
340 Duchesnay, E., “Scikit-learn: Machine learning in Python,” *Journal of Machine Learning Research* **12**,
341 2825–2830 (2011).
- 342 [35] Satterthwaite, T. D., Elliott, M. A., Ruparel, K., Loughhead, J., Prabhakaran, K., Calkins, M. E., Hop-
343 son, R., Jackson, C., Keefe, J., Riley, M., Mentch, F. D., Sleiman, P. M. A., Verma, R., Davatzikos, C.,
344 Hakonarson, H., Gur, R. C., and Gur, R. E., “Neuroimaging of the philadelphia neurodevelopmental cohort,”
345 *NeuroImage* **86**, 544–553 (2014).
- 346 [36] Farras-Permanyer, L., Mancho-Fora, N., Montalà-Flaquer, M., Bartrés-Faz, D., Vaqué-Alcázar, L., Peró-
347 Cebollero, M., and Guàrdia-Olmos, J., “Age-related changes in resting-state functional connectivity in older
348 adults,” *Neural Regen. Res.* **14**(9), 1544 (2019).
- 349 [37] Petersen, R. C., Aisen, P. S., Beckett, L. A., Donohue, M. C., Gamst, A. C., Harvey, D. J., Jack, Jr, C. R.,
350 Jagust, W. J., Shaw, L. M., Toga, A. W., Trojanowski, J. Q., and Weiner, M. W., “Alzheimer’s disease
351 neuroimaging initiative (ADNI): clinical characterization,” *Neurology* **74**, 201–209 (Jan. 2010).
- 352 [38] Sala-Llloch, R., Bartrés-Faz, D., and Junqué, C., “Reorganization of brain networks in aging: a review of
353 functional connectivity studies,” *Front. Psychol.* **6**, 663 (May 2015).
- 354 [39] Malagurski, B., Deschwanden, P. F., Jäncke, L., and Méritat, S., “Longitudinal functional connectivity
355 patterns of the default mode network in healthy older adults,” *NeuroImage* **259**, 119414 (Oct. 2022).

- 356 [40] Zonneveld, H. I., Pruijm, R. H. R., Bos, D., Vrooman, H. A., Muetzel, R. L., Hofman, A., Rombouts, S. A.,
357 van der Lugt, A., Niessen, W. J., Ikram, M. A., and Vernooij, M. W., “Patterns of functional connectivity
358 in an aging population: The rotterdam study,” *Neuroimage* **189**, 432–444 (Apr. 2019).
- 359 [41] Jolles, D. D., van Buchem, M. A., Crone, E. A., and Rombouts, S. A. R. B., “A comprehensive study of
360 whole-brain functional connectivity in children and young adults,” *Cereb. Cortex* **21**, 385–391 (Feb. 2011).

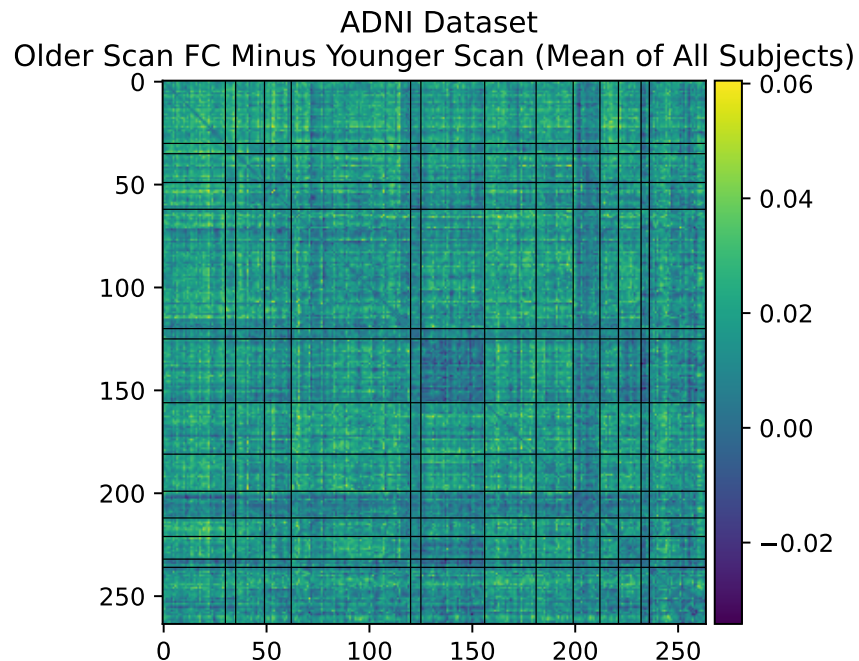


Figure 10. Mean longitudinal changes in FC between first scan and second scan in healthy controls of ADNI dataset.

APPENDIX A. LONGITUDINAL FC CHANGES IN THE ADNI DATASET

361
 362 We examined the longitudinal change in FC of healthy controls in the Alzheimer’s Disease Neuroimaging Initiative
 363 (ADNI) dataset³⁷ (age matched subjects who do not develop AD pathology). We used scans taken an average
 364 of one year apart. We confirm a small, statistically insignificant increase in total FC but fail to find the same
 365 SMT-VIS increase relative to the rest of FC as in the UKB. Statistics are given in Table 4 and the average FC
 366 change is shown in Figure 10.

| Average FC Increase | Std Dev FC Change | +Total FC | -Total FC | Total Subjects |
|---------------------|-------------------|-------------|-----------|----------------|
| 0.015 | 0.131 | 184 (52.7%) | 165 | 394 |

Table 4. There is a small but positive change in FC in ADNI healthy controls (subjects who do not go on to develop AD).

APPENDIX B. CORRELATION OF CHANGE IN FC WITH LONGITUDINAL OUTCOMES IN THE UKB

367
368

369 We identified several correlations between longitudinal change in FC and changes in clinical outcomes associated
370 with the two scan timepoints in the UKB dataset. These are presented below, along with the UKB field identifiers
371 of the outcomes. All p-values are Bonferroni-corrected with $n = 105$ multiple comparisons (one for each average
372 inter-network connectivity).

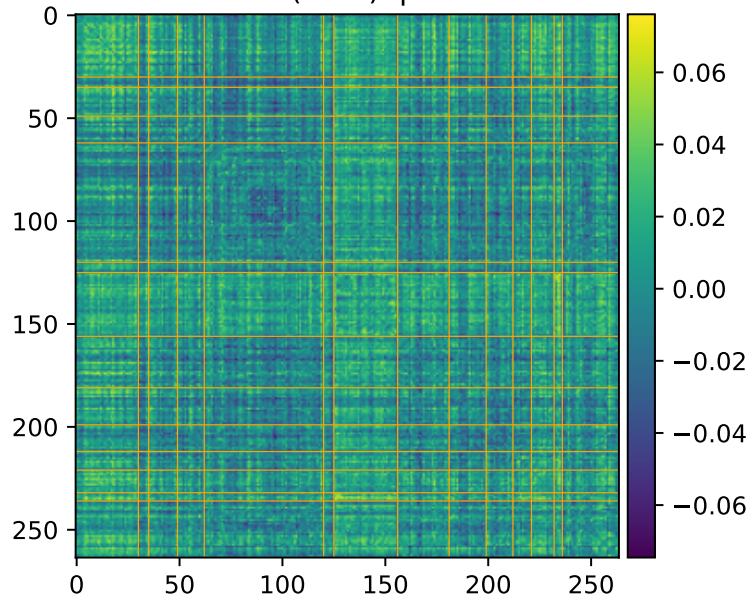
373 **B.1 SMT Hand, VIS, and CB Connectivity and Grip Strength (f.46.2.0, f.46.3.0,** 374 **f.47.2.0, f.47.3.0)**

375 We find a marginally significant association between change in hand grip strength and VIS-CB and SMT-CB
376 connectivity change (Figure 11).

377 **B.2 Body Mass Index and Basal Metabolic Rate (f.23104.2.0, f.23104.3.0, f.23105.2.0,** 378 **f.23105.3.0)**

379 We find a not statistically significant but suggestive association between BMI and basal metabolic rate change
380 and SMT-VIS connectivity change (Figure 12).

FC Change Correlation with Hand Grip Strength Change (Left)
Vis-CB (6-12): $p < 0.27$



FC Change Correlation with Hand Grip Strength Change (Right)
SMT-CB (0-12): $p < 0.09$, VIS-CB (6-12): $p < 0.56$

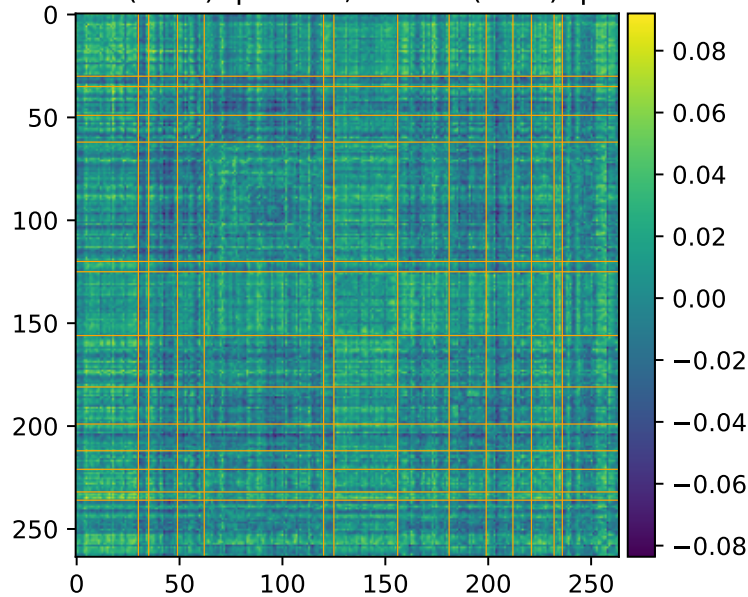
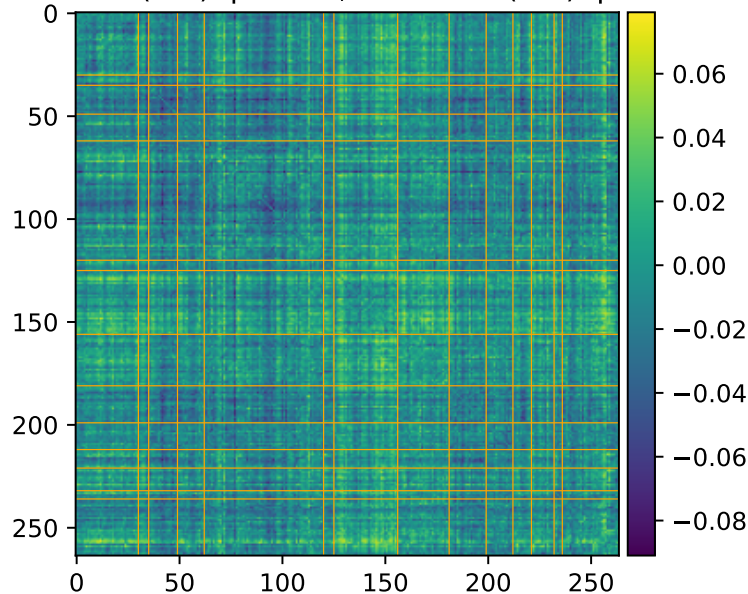


Figure 11. Hand grip strength change association with functional connectivity change in the longitudinal cohort. Bonferroni-corrected p-values.

FC Change Correlation with Body Mass Index Change
CNG-CNG (2-2): $p < 0.12$, CNG-AUD (2-3): $p < 0.76$



FC Change Correlation with Basal Metabolic Rate Change
SMT-VIS: $p < 0.05$ (Uncorrected)

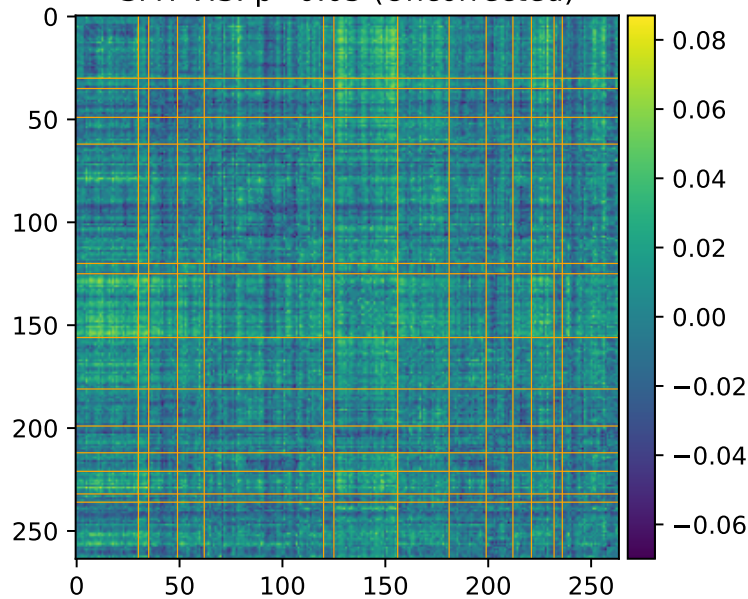


Figure 12. BMI and basal metabolic range change association with functional connectivity change in the longitudinal cohort. Bonferroni-corrected p-values.